Journal of Electronic Materials (2022) 51:1077–1088
https://doi.org/10.1007/s11664-021-09368-8

ORIGINAL RESEARCH ARTICLE

Processable GO-PANI Nanocomposite for Supercapacitor Applications

Zafer Çıplak[1]

Received: 31 July 2021 / Accepted: 23 November 2021 / Published online: 11 January 2022

Abstract
In this study, graphene oxide (GO)-polyaniline (PANI) binary nanocomposite was prepared with a facile, green, and one-step in situ polymerization approach using dodecyl benzene sulfonic acid as a dopant and stabilizing agent to achieve production of processable GO-PANI nanocomposite for supercapacitor applications. The synthesized nanocomposites were characterized with Fourier transform infrared spectroscopy, x-ray diffraction, ultraviolet–visible spectroscopy (UV–Vis), and scanning electron microscopy. The electrochemical properties of supercapacitor electrode materials were analyzed by cyclic voltammetry, galvanostatic charge–discharge, and electrochemical impedance spectroscopy (EIS) utilizing a two-electrode configuration. The effects of the amount of aniline-to GO-nanosheet ratio, used for preparation of the nanocomposite, on electrochemical performance were investigated. The GO-PANI nanocomposite demonstrated promising electrochemical performance towards supercapacitor applications. At 1 A/g current density, the GO-PANI electrodes show a high specific capacitance value of 269.3 F/g. In addition, the GO-PANI nanocomposite exhibited 81.3% specific capacitance retention after 10,000 cycles.

Keywords Graphene oxide · polyaniline · nanocomposite · supercapacitor

Introduction

The increasing demand for energy, a developing global economy, rapid depletion of fossil fuel sources, and enhancing concerns about environmental pollution make renewable energy sources a center of attraction. In recent decades, there has been a developing interest in energy storage devices for storing energy from renewable energy sources with high efficiency, low cost, and environmentally friendly nature. In addition, there is an increasing demand for energy storage systems with high energy and power densities for portable electronics.[1–6] Among other energy storage devices, supercapacitors have gained considerable attention because of their high-power density, long cycle life, and fast charge–discharge rate. The charge-storing mechanisms of supercapacitors are classified as pseudocapacitance and electrochemical double layer capacitance (EDLC).[7–9]

Electrode materials which store energy via the pseudocapacitance mechanism undergo reversible redox reactions. They are in the center of interest for supercapacitor applications because of their very high specific capacitance.[7,10] Despite their high potential and electrochemical properties, pseudocapacitance electrode materials, like conducting polymers (polyaniline, polypyrrole, etc.) and metal oxide/hydroxide nanostructures,[11] suffer from poor electrochemical performance.[7,12–15] As a widely used conducting polymer in various application areas, polyaniline (PANI) is an inexpensive and easily producible electrode material with considerably high electronic conductivity. However, morphological and mechanical properties of pristine PANI cause a low charge transfer rate, limited contribution of PANI chains to electrochemical process, and continuous swelling/shrinking during cycling, leading to low specific capacitance, low rate capability, and very limited cyclic stability.[16–18]

The production of nanocomposites of PANI with carbon-based nanostructures, such as carbon nanotubes,[19,20] reduced graphene oxide,[21–23] activated carbon,[24–26] etc. is one of the most important approaches to promote the electrochemical performance of PANI. Despite having considerably low conductivity, graphene oxide (GO) is a two-dimensional (2D) material with very high surface area and excellent mechanical strength. In addition, GO is a functional material because of having oxygen-containing groups. The abundant oxygenated functional groups of GO also contribute

✉ Zafer Çıplak
zaferciplak@cumhuriyet.edu.tr

[1] Department of Chemical Engineering, Faculty of Engineering, Sivas Cumhuriyet University, Sivas, Turkey

to the pseudocapacitance of electrodes and interaction with electrolyte ions. Additionally, GO nanosheets have excellent dispersibility in aqueous and organic solvents, which provides functionality, ease of preparation of electrode materials, improved interaction between components of the nanocomposites, and better wettability to electrodes.[27,28] As a result of these unique features, there has been a growing interest on GO-based nanocomposites for supercapacitor applications, especially for improving the electrochemical performance of metal oxide/hydroxide[29–31] and conducting polymer-containing electrode materials.[32–34]

Unlike most studies in the literature in which inorganic acids such as HCl, H_2SO_4, HNO_3, etc., were used as dopants for preparation of PANI, in this study, an organic acid, 4-dodecylbenzenesulfonic acid (DBSA), was used. DBSA functioned as both the dopant and stabilizing agent.[35,36] PANI structures doped with organic acids like DBSA,[35–37] camphor sulfonic acid (CSA),[38] *p*-toluene sulfonic acid (PTSA),[39]and methane sulfonic acid (MSA),[40] and composites of these structures, are promising pseudocapacitance electrode materials for supercapacitor applications because of their better interaction with aqueous electrolytes, wettability, stability, and processability. Because of the unique features of DBSA-doped PANI, there is a growing interest in DBSA-doped PANI-based nanocomposites, such as metal nanoparticle (Cu, Ag, Pt)-containing organic acid/inorganic acid co-doped (e.g., HCl-DBSA) nanocomposite, GO/metal nanoparticle/PANI nanocomposite,[41] and H_2SO_4-DBSA co-doped GO-PANI electrodes prepared with an interfacial polymerization approach.[42,43] In this study, the GO surface was coated with a thin film of organic acid-doped PANI in DBSA aqueous solution via a one-pot in situ polymerization technique. This study aimed to produce electrode materials having a high surface-to-volume ratio, which considerably increases the electroactive surface area of electrode materials to obtain high specific capacitance, rate capability, and electrochemical stability.

Materials and Methods

Materials

Graphite oxide was obtained from Grafen Chemical Industries (Turkey). Aniline (≥ 99.5%), ammonium persulfate (APS; ≥ 98%), and DBSA (70% in isopropanol) were supplied from Sigma-Aldrich (Germany).

Preparation of GO-PANI Nanocomposite

The GO-PANI nanocomposite samples were prepared with a facile, one-pot in situ polymerization approach. First, graphite oxide sheets were exfoliated with ultrasonication for 1 h to produce GO aqueous dispersion (0.5 mg/mL). Then, DBSA (0.1 M) was added dropwise on the as-prepared GO aqueous dispersion. Aniline monomer was dissolved in 0.1 M DBSA aqueous solution at room temperature, then added to the above GO dispersion and stirred for 2 h to achieve a homogenous distribution of monomer on GO nanosheets. Finally, APS (APS/aniline 1:1 n/n) was added in GO-aniline mixture for oxidation of aniline monomer to achieve polymerization of PANI on the GO surface. The mixture was kept at room temperature and stirred overnight. Absolute ethanol was added to the obtained highly stable GO-PANI dispersion to precipitate the nanocomposite. The precipitated sample was mixed and centrifuged with deionized (DI) water and absolute ethanol four times to remove excess aniline and oligomeric structures. The purified nanocomposite samples were dried in a vacuum oven at 60°C for further characterizations and electrochemical measurements. In addition, the effects of PANI coating on GO nanosheets were investigated via production of samples with different GO/aniline monomer weight ratios.

The nanocomposites prepared with different weight ratios [aniline/GO 1.5–16 (w/w)] and the samples were marked as GO-PANI1.5, GO-PANI4, GO-PANI8, and GO-PANI16, respectively.

Material Characterization

The structural characterizations of the samples were carried out with Fourier transform infrared (FT-IR) spectroscopy between 600 cm^{-1} and 4000 cm^{-1} (Shimadzu FTIR 8400-S FTIR), ultraviolet–visible (UV–Vis) spectroscopy between 200 nm and 900 nm (Shimadzu 1601 UV–Vis spectrophotometer). The crystal structures of the samples were investigated with x-ray diffraction (XRD). XRD patterns were obtained with a Rigaku MiniFlex 600 x-ray diffractometer with CuKα radiation in a 2θ range from 5° to 80°. The surface and morphological characterizations of the samples were performed via field-emission scanning electron microscopy (FE-SEM) (FEI QUANTA 400F).

Electrode Preparation and Electrochemical Measurements

The electrochemical measurements utilized a two-electrode coin cell. All measurements were carried out in 1 M H_2SO_4 electrolyte. Electrochemical measurements were performed with a Gamry Reference 3000 potentiostat/galvanostat electrochemical work station by performing galvanostatic charge/discharge (GCD), cyclic voltammetry (CV), and electrochemical impedance spectroscopy (EIS) analyses. The CV measurements were carried out between 0 V and 0.8 V at various scan rates between 5 mV/s and 200 mV/s. GCD measurements were done

between 0 V and 0.8 V at different applied current densities between 1 A/g and 5 A/g. EIS analysis was carried out with frequency rate from 150 kHz to 0.01 Hz. Coin-shaped stainless-steel plates with a surface area of 1 cm^2 were used as current collectors. The working electrodes were produced by coating of homogenous slurry of GO-PANI nanocomposite (80%) with carbon black (15 wt.%) and polyvinylidene fluoride (PVDF) (5 wt.%) in N-methylpyrrolidone (NMP) on the stainless-steel current collectors. The prepared electrodes were dried in a vacuum oven at 70°C for 24 h.

For a symmetrical two-electrode configuration, the specific capacitance of the electrodes was calculated with Eq. 1 using CV curves of the electrodes.

$$C = \frac{2\int IdV}{\nu m \Delta V} \tag{1}$$

where C (F/g) is the capacitance of per electrode, m (g) is the mass of the electrode material coated on a single working electrode, ν (mV/s) is the scan rate, and ΔV (V) is the potential window.[44]

The specific capacitance was also calculated with the discharge portion of the GCD curves according to Eq. 2.[45]

$$C = \frac{2I\Delta t}{m\Delta V} \tag{2}$$

where ΔV (V) is the applied potential difference excluding IR drop, I (A) is applied current, and Δt (s) is the discharge time.

Results

Characterization of the Electrode Materials

The binary GO-PANI nanocomposite was prepared with a one-pot in situ polymerization approach as represented in Fig. 1. The chemical structure of GO nanosheets shows existence of plenty of hydroxyl, carboxyl, and epoxy oxygenated functional groups, which gives GO a strong hydrophilic nature that provides excellent dispersibility in water. In addition, the 2D structure and very high surface area of aromatic GO nanosheets ensure strong π–π attraction between aniline molecules and GO, providing effective loading of monomer. Moreover, electrostatic attraction forces and hydrogen bonding between aniline and GO nanosheets are also helpful for strong interaction of as-prepared PANI with GO.[32] This interaction is crucial to achieve high electrochemical performance. Owing to its high surface area and having plenty of active centers, GO also can be considered as a template for in situ polymerization of PANI. It is expected to form an ultrafine polymeric structure on the surface of GO nanosheets after polymerization in DBSA aqueous solution with the help of a strong oxidizing agent APS. The effects of aniline monomer amount [GO/aniline 1.5–16 (w/w)] that was used for production of the nanocomposites on chemical, morphological, and electrochemical properties of the samples were investigated.

Figure 2a shows UV–Vis spectrum of GO nanosheets. The band at 230 nm corresponds to $\pi \rightarrow \pi^*$ transition of aromatic C–C bonds of GO. The other band at ~300 nm is attributed to $n \rightarrow \pi^*$ transition of C=O bonds. The UV–Vis

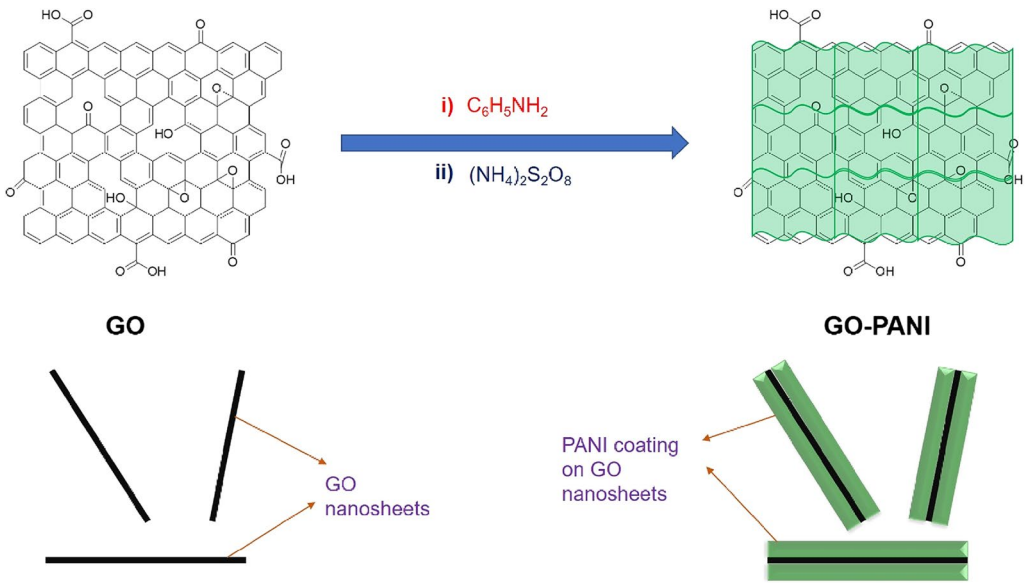

Fig. 1 Schematic representation of preparation of GO-PANI nanocomposite.

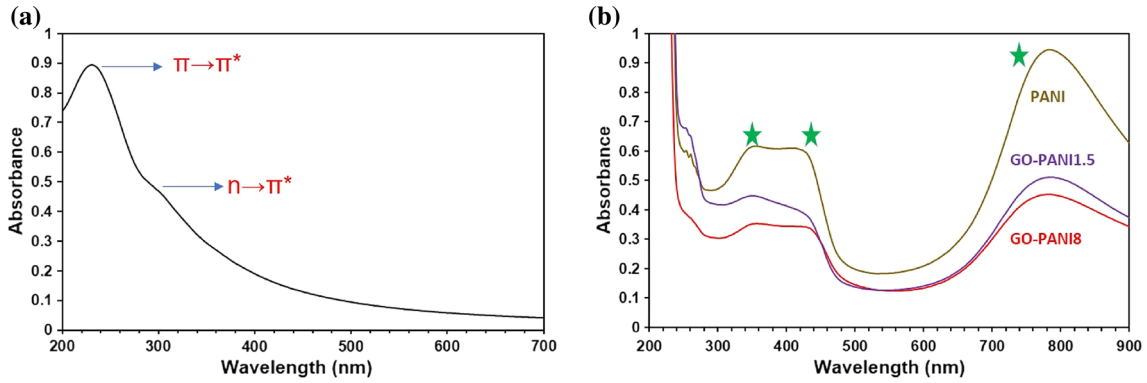

Fig. 2 UV–Vis spectrum of (a) GO, (b) pristine PANI, GO-PANI1.5, and GO-PANI8.

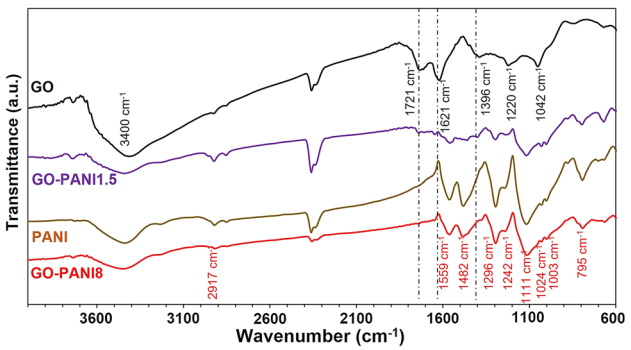

Fig. 3 FTIR spectrum of GO, PANI, GO-PANI1.5, and GO-PANI8.

spectra of pristine PANI and GO-PANI samples introduce three characteristic bands of the protonated emeraldine salt form of PANI. The first band at between 325 nm and 360 nm is attributed to π–π^* transition of the benzenoid ring. The second band between 400 nm and 430 nm is due to polaron–π^* transitions. The third characteristic band is the broad peak at about 750–800 nm that corresponds to interchain excitation[46] (Fig. 2b). The UV–Vis spectra of GO-PANI nanocomposites indicate successful coating of GO nanosheets by the PANI polymeric structure.

Figure 3 displays FTIR spectra of GO, PANI, GO-PANI1.5, and GO-PANI8 samples. GO is abundant with oxygenated functional groups of carboxyl, hydroxyl, epoxy, etc. The FTIR spectrum of GO contains characteristic bands at about 3400 and 1396 cm^{-1} correspond to O–H stretching vibration and C–OH deformation, respectively. The peak at 1721 cm^{-1} is attributed to C=O stretching vibration, and the band at 1621 cm^{-1} arises from C=C stretching of unoxidized sp^2 domains of graphite. The peaks at about 1220 cm^{-1} and 1042 cm^{-1} are attributed to C–O (epoxy) and C–OH (alkoxy) peaks, respectively. The FTIR spectrum of the PANI sample doped with DBSA has the emeraldine salt form of the polymeric structure and contains the characteristic bands at about 3000–3600 cm^{-1}, 1559 cm^{-1}, 1482 cm^{-1}, 1296 cm^{-1}, 1111 cm^{-1}, and 795 cm^{-1}. These characteristic peaks correspond to protonated imines ($–NH^+$) and amines ($–NH^–$) of PANI chains, quinoid ring deformations, benzenoid ring deformations, C–N, C–N^+, N–H^+= stretching vibrations, and plane stretching of C–H bonds, respectively. Moreover, the PANI sample also possesses peaks of C–H stretching (2917 cm^{-1}), S=O (1024 cm^{-1}), and $>CH_2$ (1003 cm^{-1}) stretching vibrations of DBSA. As a result of effective coating of GO nanosheets by PANI polymeric structure, the binary GO-PANI nanocomposite samples exhibit all the characteristic bands of the emeraldine salt form of PANI. Besides, the FTIR spectrum of the nanocomposite sample prepared with the lowest amount of aniline monomer (GO-PANI1.5) also exhibits various bands of GO nanosheets in addition to the characteristic peaks of DBSA-doped PANI. These bands are C=O stretching vibration (1741 cm^{-1}), C–OH deformation (1404 cm^{-1}), and C=C stretching (1651 cm^{-1}). Additionally, for the nanocomposite sample, the redshift of the C=O band from 1721 cm^{-1} to 1741 cm^{-1}, C–OH deformation from 1396 cm^{-1} to 1404 cm^{-1}, and C=C stretching from 1621 cm^{-1} to 1651 cm^{-1} indicates strong interaction between PANI chains and GO nanosheets, which is also of key importance to achieve high electrochemical performance. This strong interaction between the GO and polymeric structure may originate because of the π–π stacking, electrostatic interaction, and hydrogen bonding.

Figure 4a presents the XRD diffraction pattern of GO. The GO sample has a strong peak at about 10.74° corresponding to a (002) planar reflection of GO layers, having d-spacing of 0.822 nm between nanosheets.[47] Figure 4b shows XRD diffraction patterns of PANI, GO-PANI1.5, and GO-PANI8. The pristine PANI has characteristic bands at 14.6°, 20.7°, and 25.4° attributed to (011), (020), and (200) crystal planes of PANI, respectively, which indicates the polymer sample has a crystalline structure. The diffraction patterns of GO-PANI nanocomposites have similar features with PANI and possess the characteristic peaks of crystal planes of PANI, while the (002) planar reflection peak of GO

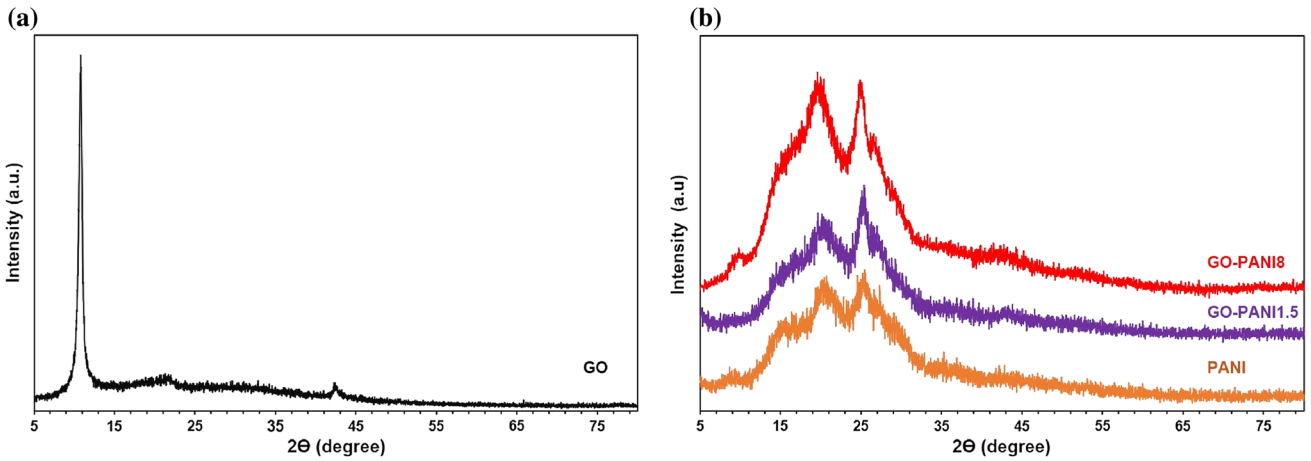

Fig. 4 XRD diffraction patters of (a) GO, (b) PANI, GO-PANI1.5, and GO-PANI8.

disappeared. This finding indicates that the polymeric structure prepared with an in situ polymerization approach on GO nanosheets maintains its crystalline nature. In addition, the homogenous coating and production of PANI ultrafine films between GO nanolayers caused complete separation of GO nanosheets.[48,49]

Figure 5 shows SEM images of GO, PANI, GO-PANI1.5, GO-PANI8, and GO-PANI16 samples. The GO nanosheets have a wrinkled and corrugated platelet structure, consisting of a few layers of graphene sheets (Fig. 5a). The pristine PANI sample has an interconnected structure containing sub-micron polymeric particles (Fig. 5b). SEM images of GO-PANI1.5 demonstrate a structure of interconnected PANI nanoparticles on GO nanosheets with a minority of uncoated surfaces of GO layers (Fig. 5c). Increasing the aniline amount led to uniform coating of GO platelets (GO-PANI8) and formation of ultrafine polymer films on the 2D layers, which have a smooth surface. It is noticed that the nanocomposite samples have a different texture in comparison to pristine PANI. The high surface area, the presence of plenty of active centers, and strong interactions between aniline monomer and GO layers caused formation of very small interconnected PANI nanoparticles which are smaller compared to pristine PANI sub-micron particles (GO-PANI1.5) (Fig. 5d). The increase of aniline amount in the reaction caused growth of those small nanoparticles to form an ultrafine smooth film on GO nanosheets. The surfactant role of DBSA molecules may restrict further growth of the polymeric film which also depends on the ratio of aniline/GO used for production of the nanocomposites. However, further increase in the aniline/GO ratio (GO-PANI16) caused thickening of the polymeric film on GO nanosheets and even formation of an interconnected structure of PANI layers (Fig. 5e). Figure 5f displays a transmission electron microscopy (TEM) image of GO-PANI8 nanocomposite. Similar to SEM images, the TEM image also shows the nanocomposite has a film structure consisting of ultrafine polymer coating on GO nanosheets. The SEM and TEM images confirm the chemical characterization of the samples and exhibit strong interaction between PANI and GO nanosheets and successful preparation of the ultrafine PANI polymeric films on the GO surface.

Electrochemical Measurements of Electrodes

The electrochemical performance of the GO, PANI, and GO-PANI binary nanocomposite samples were investigated in a two-electrode configuration. The two-electrode configuration has a physical configuration and charge transfer mechanism similar to practical supercapacitors that exhibit the exact performance of the electrode materials accurately.[50,51] All measurements were carried out in 1 M H_2SO_4 electrolyte in a potential window between 0 V and 0.8 V. Figure 6 shows CV curves of GO, PANI, GO-PANI1.5, GO-PANI4, GO-PANI8, and GO-PANI16 samples at a scan rate of 10 mV/s. According to Eq. 1, the integrated area in the CV curves of the electrodes is directly proportional to the specific capacitance. Based on Eq. 1, GO, GO-PANI1.5, PANI, GO-PANI4, GO-PANI8, and GO-PANI16 exhibit specific capacitance values of 12.5 F/g, 164 F/g, 297.8 F/g, 412.5 F/g, 510.5 F/g, and 391.7 F/g, respectively. The GO electrodes have the lowest specific capacitance because of the poor electronic conductivity of GO nanosheets. Compared to pristine PANI doped with DBSA, GO-PANI1.5 displays lower specific capacitance due to inadequate coating of PANI and the existence of a low amount of polymeric structure as the active electrode material. The increase of aniline/GO ratio promoted the electrochemical performance of the nanocomposite, and the GO-PANI8 sample demonstrated the highest specific capacitance. However, the further

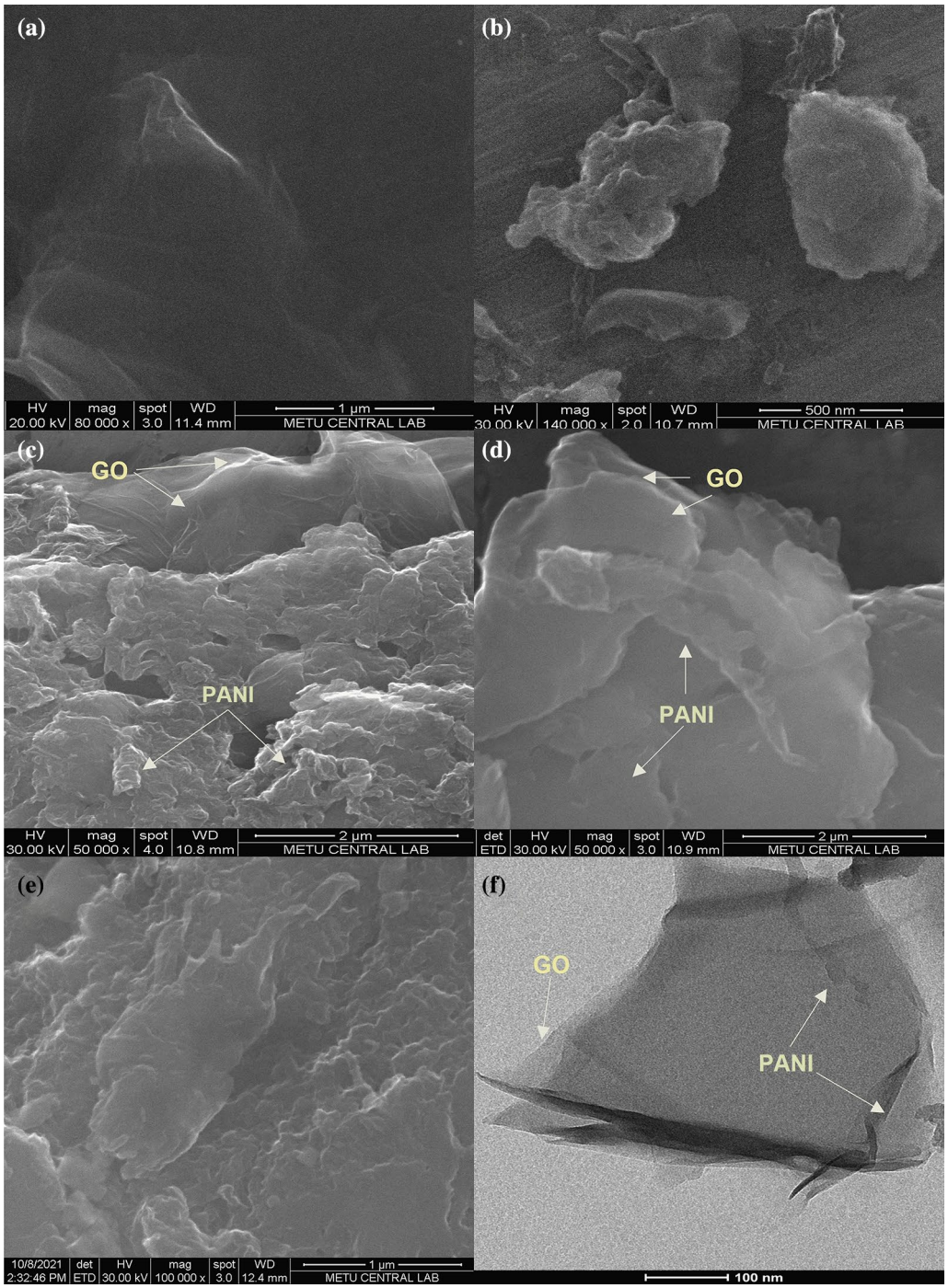

Fig. 5 SEM images of (a) GO (b) PANI, (c) GO-PANI1.5, (d) GO-PANI8, and (e) GO-PANI16; (f) TEM image of GO-PANI8.

increase of aniline/GO ratio (GO-PANI16) decreased the specific capacitance. Being a pseudocapacitive electrode material, the reversible redox reactions of PANI are the main driving force to create electrochemical performance. The increase of the aniline/GO ratio also caused the increment of PANI film thickness coating the GO nanosheets. The increase of the polymeric film thickness at high values of aniline/GO ratio also increases the ion diffusion path of electrolyte ions that diminish the specific capacitance of electrodes.

Figure 7 displays the effect of sweep rate (5–200 mV/s) on the electrochemical performance of PANI and GO-PANI8 electrodes. The morphological structure, ionic conductivity, and electrolyte–electrode interaction of the

electrodes are crucial factors, which designate ion diffusion properties and rate capability of the supercapacitors. As an ideal supercapacitor behavior, both PANI and GO-PANI8 electrodes exhibit enhanced current responses with the increased scan rate. Additionally, both supercapacitor cells display a quasi-rectangular shape with two redox couples of PANI. The redox couple at about 0.2 V is attributed to leucoemeraldine/emeraldine transformation, and the redox couple at about 0.5 V is referred to emeraldine/pernigraniline transition. The GO-PANI8 nanocomposite electrode retains its quasi-rectangular shape and the redox couples of PANI. They are still apparent even at the highest applied sweep rate, which proves the high electrochemical stability of GO-PANI8 nanocomposite. The increase of the scan rate causes restrictions and limits the accessibility of the electrolyte ions into the electrode material. At higher sweep rates, only the surface parts of the electrode material participate in the electrochemical process effectively. Due to this diffusion restriction, ions cannot reach inner parts of the electrode material, which decreases the specific capacitance. Figure 7c shows the dependence of the specific capacitance of PANI and GO-PANI8 on the applied scan rate (5–200 mV/s). GO-PANI8 and PANI electrodes retained 81.6% and 50.0% of their specific capacitances in this sweep rate range, respectively. Pristine PANI doped with DBSA has an interconnected structure of sub-micron particles, which causes PANI electrodes to suffer from high charge diffusion restrictions and limited participation of the inner PANI chains in the electrochemical process, which diminishes the rate capability and specific capacitance values at higher applied scan rates. In comparison to PANI, GO-PANI8 nanocomposite has an excellent rate capability. The ultrafine PANI coating on GO platelets decreases the ion diffusion path and leads

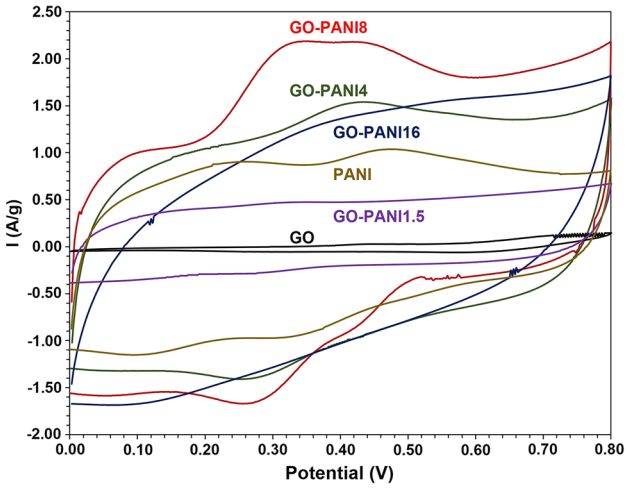

Fig. 6 CV curves of GO, PANI, GO-PANI1.5, GO-PANI4, GO-PANI8, and GO-PANI16 at a scan rate of 10 mV/s in 1 M H_2SO_4 electrolyte.

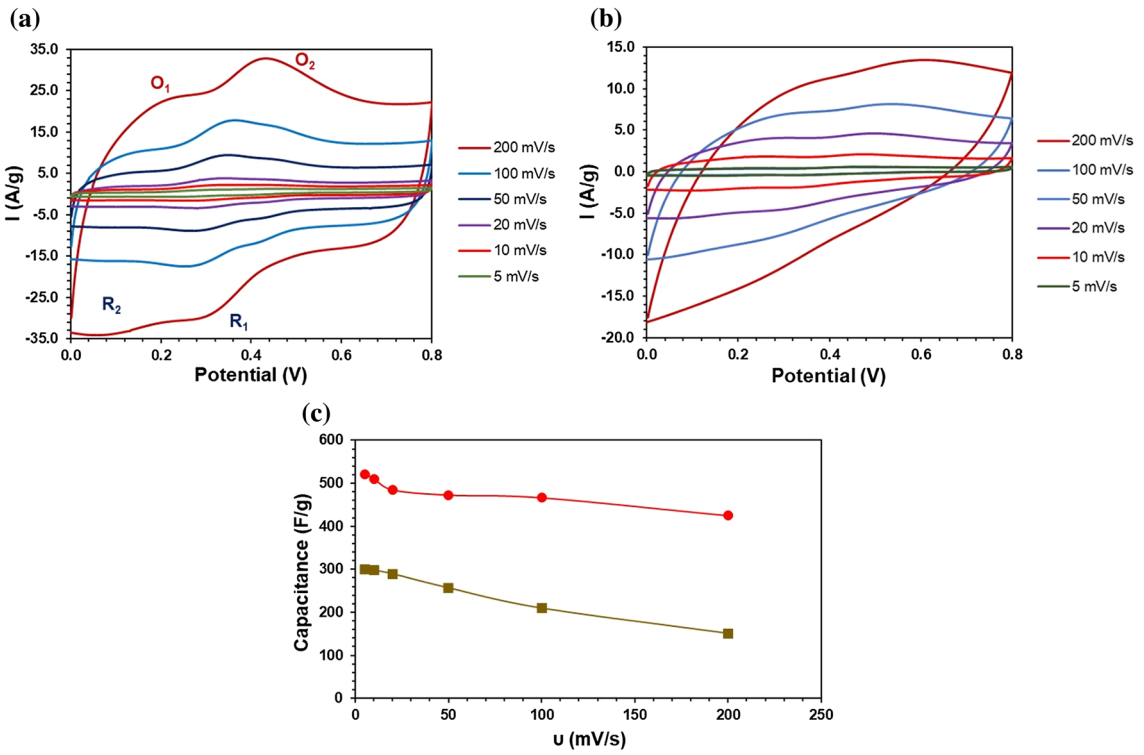

Fig. 7 CV curves of (a) GO-PANI8 and (b) PANI electrodes at various scan rates of 5–200 mV/s; (c) dependence of specific capacitance on scan rate (5–200 mV/s) for GO-PANI8 and PANI.

to fast penetration of electrolyte ions, which results in more effective participation of PANI chains in reversible redox reactions in order to retain electrochemical performance even at high sweep rates.

Figure 8a represents GCD curves of GO, GO-PANI1.5, GO-PANI4, GO-PANI8, and GO-PANI16 samples at a current density of 1 A/g. According to Eq. 2, the obtained specific capacitance values for GO, GO-PANI1.5, PANI, GO-PANI16, GO-PANI4, and GO-PANI8 electrodes are 9.6 F/g, 72.8 F/g, 180.5 F/g, 193.3 F/g, 206.5 F/g, and 269.3 F/g, respectively. Figure 8b shows GCD curves of GO-PANI8 nanocomposite at various applied current densities (1–5 A/g). At 1 A/g, 2 A/g, and 5 A/g current densities, the GO-PANI8 electrodes exhibited specific capacitance values of 269.3 F/g, 259.2 F/g, and 251.7 F/g, respectively. Similarly, with CV analysis, between 1 A/g and 5 A/g current densities, the GO-PANI8 retained 93.5% of its specific capacitance, which indicates that the binary GO-PANI8 nanocomposite doped with DBSA has an excellent rate capability. The cyclic stability of the electrodes is another essential parameter for supercapacitor electrode materials. The conducting polymer-based supercapacitor electrodes suffer from structural deterioration, corresponding to a dramatic decrease of electrochemical performance due to swelling and shrinking of polymer chains during the repetitive charge–discharge process. On the other hand, after 10,000 charge–discharge cycles at a current density of 2 A/g, the GO-PANI8 electrodes exhibited a capacitive retention value of 81.3%. The GO-PANI8 nanocomposite doped with DBSA exhibited a high cyclic stability because of excellent mechanical strength of GO nanosheets; the formation of a compact nanocomposite structure is attributed to strong interactions between ultrafine PANI film and GO.

EIS is an important technique to determine charge transfer properties of electrode materials. Figure 9a and b displays Nyquist plots of PANI, GO-PANI1.5, GO-PANI4, and GO-PANI8, and Fig. 9c shows the equivalent circuit fitting the EIS data. The equivalent circuit is composed of equivalent series resistance (R_s), charge transfer resistance (R_{CT}), Warburg impedance (Z_w), double layer capacitance (C_{dl}), and pseudocapacitance (C_{ps}).[52,53] The Nyquist plots of the electrodes consist of two main parts: (1) the semicircle corresponding to charge transfer resistance (R_{CT}) of the electrode material in the high-frequency region and (2) the straight line in the low-frequency region related to the ion transfer rate to the electrode material. For GO-PANI1.5, PANI, GO-PANI4, and GO-PANI8 electrodes, the R_{CT} values were determined to be 19.38 Ω, 3.27 Ω, 2.17 Ω, and 0.79 Ω, respectively. The lower R_{CT} value for GO-PANI8 electrodes indicates improved charge transport compared to pristine PANI and other nanocomposite samples. Moreover, in the low-frequency region, the slope of the vertical line of

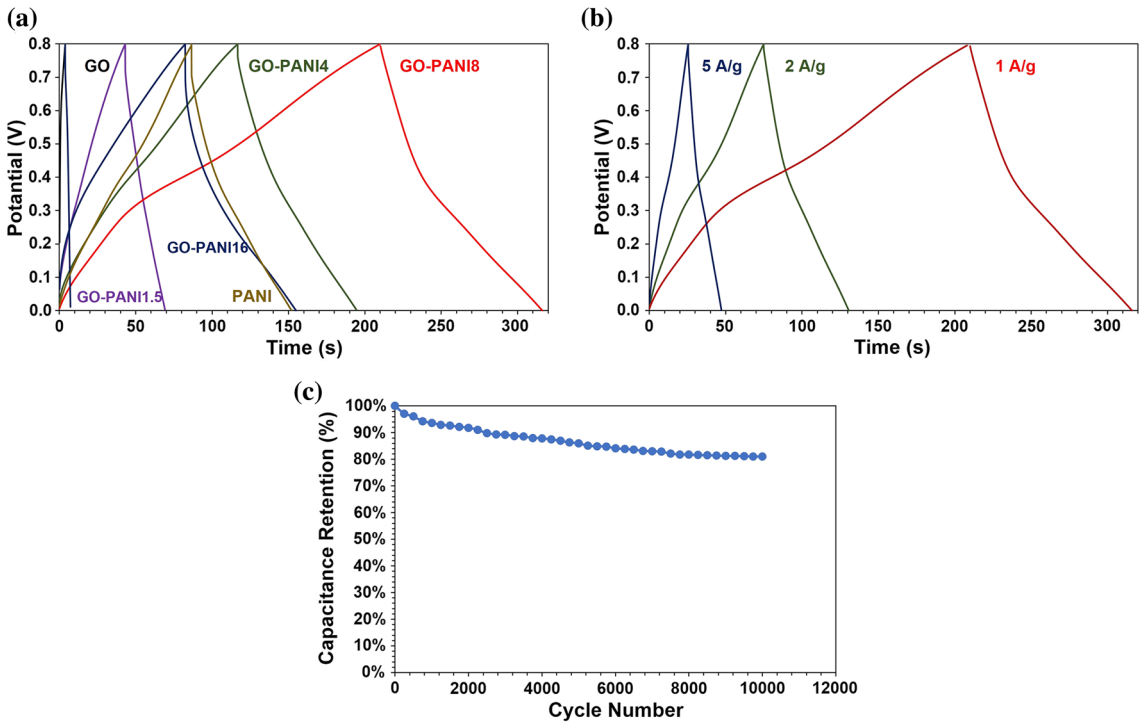

Fig. 8 (a) GCD curves of GO, GO-PANI1.5, GO-PANI4, GO-PANI8, and GO-PANI16 electrodes at applied current density of 1 A/g in 1 M H_2SO_4 electrolyte, (b) GCD curves of GO-PANI8 electrodes at various scan rates (1–5 A/g), (c) cyclic stability of GO-PANI8 nanocomposite.

GO-PANI8 nanocomposite is greater than other electrodes, which indicates GO-PANI8 exhibits faster ion transport to electrode material and a more ideal capacitor behavior compared to other electrodes.[54,55] The Nyquist plots of the samples show that GO-PANI8 has better charge transfer properties, in addition to its high specific capacitance, excellent rate capability, and electrochemical stability. The strong interaction and synergistic effects between PANI and GO nanosheets, the ultrafine PANI film formation on GO nanoplatelets, and the effective doping agent and surfactant role of DBSA molecules contribute to the electrochemical performance of the GO-PANI binary nanocomposite. Moreover, the organic acid doping of PANI polymeric structure is also helpful for homogenous coating of current collectors during electrode preparation because of good dispersibility of electrode material in NMP.

Table I presents a comparison of the electrochemical performance of DBSA-doped GO-PANI nanocomposite with some studies including GO-PANI structures in the literature, in which inorganic acids were used as doping agents for production of PANI. The organic acid (DBSA)-doped GO-PANI nanocomposite exhibited superior electrochemical performance compared to many studies based on inorganic acid-doped GO-PANI electrodes. Compared to its inorganic acid-doped counterparts, the promising electrochemical performance of DBSA-doped GO-PANI electrodes may arise from their better processability, homogenous coating, wettability, and better interaction with aqueous electrolyte. The results demonstrate organic acid-doped conducting polymers are also candidates having high potential for supercapacitor application.

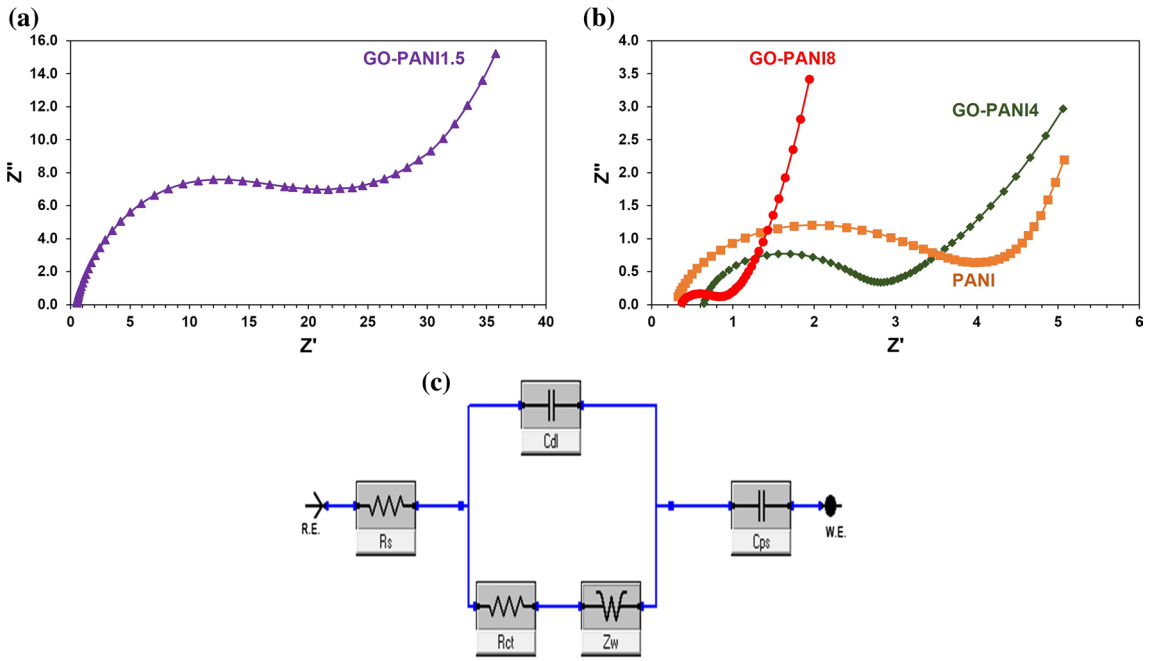

Fig. 9 (a) Nyquist plot of GO-PANI1.5 nanocomposite, (b) Nyquist plots of PANI, GO-PANI4, and GO-PANI8 electrodes, and (c) equivalent circuit model fitting the EIS data.

Table I Specific capacitance of GO-PANI nanocomposite-based electrode materials in the literature.

Electrode material	Dopant acid	Electrode configuration	Specific capacitance	References
GO-PANI	H_2SO_4-DBSA	Three-electrode	264 F/g at 1 A/g	42
GO-PANI	HCl	Three-electrode	42 F/g at 0.4 A/g	56
PANI/GO	H_2SO_4	Three-electrode	275 F/g at 20 mV/s	48
GO/PANI/PVDF	HCl	Three-electrode	170.63 F/g at 10 mV/s	57
PANI-GO	H_2SO_4	Three-electrode	504 F/g at 10 mV/s	58
GO/PANI	$HClO_4$	Two-electrode	150 F/g at 10 mV/s	59
GO-PANI	H_2SO_4	Two-electrode	100 F/g at 0.6 A/g	60
GO-PANI	DBSA	Two-electrode	269.3 F/g at 1 A/g	This study

Discussion

In summary, GO-PANI nanocomposite was prepared with a green, facile, one-pot approach in DBSA aqueous solution using various aniline/GO ratios [aniline/GO 1.5–16 (w/w)]. The GO nanosheets were uniformly coated with an ultrafine PANI polymeric structure by tuning the aniline/GO ratio. In a two-electrode configuration, GO-PANI8 nanocomposite sample exhibited a specific capacitance value of 269.3 F/g and retained 81.3% of its specific capacitance after 10,000 consecutive charge–discharge cycles at 1 A/g applied current density. The results indicate organic acid-doped conducting polymer-based nanocomposites are promising electrode materials for energy storage applications.

Acknowledgment The authors thank the Scientific and Technological Research Council of Turkey (TÜBİTAK; Project No. 115M456) for financial support.

Conflict of interest Zafer Çıplak declares that he has no conflict of interest.

References

1. S. Kumar, G. Saeed, L. Zhu, K.N. Hui, N.H. Kim, and J.H. Lee, 0D to 3D Carbon-Based Networks Combined with Pseudocapacitive Electrode Material for High Energy Density Supercapacitor: A Review. *Chem. Eng. J.* 403, 126352 (2021).
2. Q.Q. Xiong, and Z.G. Ji, Controllable Growth of MoS_2/C Flower-like Microspheres with Enhanced Electrochemical Performance for Lithium Ion Batteries. *J. Alloys Compd.* 673, 215 (2016).
3. S. Shen, R. Zhou, Y. Li, B. Liu, G. Pan, Q. Liu, Q. Xiong, X. Wang, X. Xia, and J. Tu, Bacterium, Fungus, and Virus Microorganisms for Energy Storage and Conversion, Small. *Methods* 3, 1900596 (2019).
4. Y.Q. Zheng, Y.F. Yuan, Z.W. Tong, H. Yin, S.M. Yin, and S.Y. Guo, Watermelon-like TiO_2 Nanoparticle (P25)@microporous Amorphous Carbon Sphere with Excellent Rate Capability and cycling performance for Lithium-Ion Batteries. *Nanotechnology* 31, 215407 (2020).
5. Z. Zhao, X. Teng, Q. Xiong, H. Chi, Y. Yuan, H. Qin, and Z. Ji, Nano-sized $FeSe_2$ Decorated RGO as a Potential Anode Material with Enhanced Lithium-Ion Storage. *Sustain. Mater. Technol.* 29, e00313 (2021).
6. J. Ren, Y. Huang, H. Zhu, B. Zhang, H. Zhu, S. Shen, G. Tan, F. Wu, H. He, S. Lan, X. Xia, and Q. Liu, Recent Progress on MOF-Derived Carbon Materials for Energy Storage. *Carbon Energy* 2, 176 (2020).
7. W. Raza, F. Ali, N. Raza, Y. Luo, K.-H. Kim, J. Yang, S. Kumar, A. Mehmood, and E.E. Kwon, Recent Advancements in Supercapacitor Technology. *Nano Energy* 52, 441 (2018).
8. Q. Xiong, C. Zheng, H. Chi, J. Zhang, and Z. Ji, Reconstruction of TiO_2/MnO_2-C Nanotube/Nanoflake Core/Shell Arrays as High-Performance Supercapacitor Electrodes. *Nanotechnology* 28, 405 (2017).
9. Q. Guo, N. Chen, and L. Qu, Two-dimensional Materials of Group-IVA Boosting the Development of Energy Storage and Conversion. *Carbon Energy* 2, 54 (2020).
10. P. Naskar, A. Maiti, P. Chakraborty, D. Kundu, B. Biswas, and A. Banerjee, Chemical Supercapacitors: A Review Focusing on Metallic Compounds and Conducting Polymers. *J. Mater. Chem. A* 9, 1970 (2021).
11. X. Xia, Y. Zhang, D. Chao, C. Guan, Y. Zhang, L. Li, X. Ge, I.M. Bacho, J. Tu, and H.J. Fan, Solution Synthesis of Metal Oxides for Electrochemical Energy Storage Applications. *Nanoscale* 6, 5008 (2014).
12. D. Majumdar, Review on Current Progress of MnO_2-Based Ternary Nanocomposites for Supercapacitor Applications. *ChemElectroChem* 8, 291 (2021).
13. D. Yiğit, F. Soysal, T. Güngör, B. Çiçek, and M. Güllü, Carbon Nanofiber/Poly(Tetrahydro[1,4]Dioxino[2,3-B]Thieno[3,4-E][1,4]Dioxine) Binder-Free Composite Redox-Active Electrode for Electrochemical Energy Storage Applications. *RSC Adv.* 7, 41419 (2017).
14. S. Khan, A. Majid, and R. Raza, Synthesis of PEDOT: PPy/AC Composite as an Electrode for Supercapacitor. *J. Mater. Sci. Mater. Electron.* 31, 13597 (2020).
15. J.B. Wu, R.Q. Guo, X.H. Huang, and Y. Lin, Construction of Self-supported Porous TiO_2/NiO Core/Shell Nanorod Arrays for Electrochemical Capacitor Application. *J. Power Sources* 243, 317 (2013).
16. H. Li, J. Wang, Q. Chu, Z. Wang, F. Zhang, and S. Wang, Theoretical and Experimental Specific Capacitance of Polyaniline in Sulfuric Acid. *J. Power Sources* 190, 578 (2009).
17. A. Eftekhari, L. Li, and Y. Yang, Polyaniline Supercapacitors. *J. Power Sources* 347, 86 (2017).
18. X. Xia, D. Chao, X. Qi, Q. Xiong, Y. Zhang, J. Tu, H. Zhang, and H.J. Fan, Controllable Growth of Conducting Polymers Shell for Constructing High-Quality Organic/Inorganic Core/Shell Nanostructures and Their Optical-Electrochemical Properties. *Nano Lett.* 13, 4562 (2013).
19. Y.Z. Cai, Y.S. Fang, W.Q. Cao, P. He, and M.S. Cao, MXene-CNT/PANI Ternary Material with Excellent Supercapacitive Performance Driven by Synergy. *J. Alloys Compd.* 868, 159159 (2021).
20. N.R. Aswathy, S.A. Kumar, S. Mohanty, S.K. Nayak, and A.K. Palai, Polyaniline/Multi-walled Carbon Nanotubes Filled Biopolymer Based Flexible Substrate Electrodes for Supercapacitor Applications. *J. Energy Storage* 35, 102256 (2021).
21. A. Moyseowicz, and G. Gryglewicz, Hydrothermal-Assisted Synthesis of a Porous Polyaniline/Reduced Graphene Oxide Composite as a High-Performance Electrode Material for Supercapacitors. *Compos. Part B Eng.* 159, 4 (2019).
22. K. Gholami Laelabadi, R. Moradian, and I. Manouchehri, One-Step Fabrication of Flexible, Cost/Time Effective, and High Energy Storage Reduced Graphene Oxide@PANI Supercapacitor. *ACS Appl. Energy Mater.* 3, 5301 (2020).
23. R. Jain, R. Mehrotra, and S. Mishra, Synthesis of B Doped Graphene/Polyaniline Hybrids for High-Performance Supercapacitor Application. *J. Mater. Sci. Mater. Electron.* 30, 2316 (2019).
24. S. Acharya, S. Sahoo, S. Sonal, J.H. Lee, B.K. Mishra, and G.C. Nayak, Adsorbed Cr(VI) Based Activated Carbon/Polyaniline Nanocomposite: A Superior Electrode Material for Asymmetric Supercapacitor Device. *Compos. Part B Eng.* 193, 107913 (2020).
25. A. Chonat, and S. Palatty, Enhanced Electrochemical Performance of a Hybrid Supercapacitive Material Based on Ternary Doped Polyaniline/Activated Carbon Composite. *Energy Fuels* 34, 10148 (2020).
26. X. Zhang, S. Yang, Y. Jiang, D. An, J. Huang, D. Chen, Y. Zhang, F. Yu, and Y. Chen, Multi-dimensional Graded Electrodes with Enhanced Capacitance and Superior Cyclic Stability. *J. Power Sources* 481, 228911 (2021).
27. Y. Zhang, L. Si, B. Zhou, B. Zhao, Y. Zhu, L. Zhu, and X. Jiang, Synthesis of Novel Graphene Oxide/Pristine Graphene/

Polyaniline Ternary Composites and Application to Supercapacitor. *Chem. Eng. J.* 288, 689 (2016).
28. Y. Tian, Z. Yu, L. Cao, X.L. Zhang, C. Sun, and D.W. Wang, Graphene Oxide: An Emerging Electromaterial for Energy Storage and Conversion. *J. Energy Chem.* 55, 323 (2021).
29. Z.Q. Wen, M. Li, F. Li, S.J. Zhu, X.Y. Liu, Y.X. Zhang, T. Kumeria, D. Losic, Y. Gao, W. Zhang, and S.X. He, Morphology-Controlled MnO_2-Graphene Oxide-Diatomaceous Earth 3-Dimensional (3D) Composites for High-Performance Supercapacitors. *Dalt. Trans.* 45, 936 (2016).
30. P. Asen, S. Shahrokhian, and A. Irajizad, One Step Electrodeposition of V_2O_5/Polypyrrole/Graphene Oxide Ternary Nanocomposite for Preparation of a High Performance Supercapacitor. *Int. J. Hydrog. Energy* 42, 21073 (2017).
31. D. Deng, N. Chen, X. Xiao, S. Du, and Y. Wang, Electrochemical Performance of CeO_2 Nanoparticle-Decorated Graphene Oxide as an Electrode Material for Supercapacitor. *Ionics (Kiel).* 23, 121 (2017).
32. T.-W. Chang, L.-Y. Lin, P.-W. Peng, Y.X. Zhang, and Y.Y. Huang, Enhanced Electrocapacitive Performance for the Supercapacitor with Tube-like Polyaniline and Graphene Oxide Composites. *Electrochim. Acta* 259, 348 (2018).
33. A. Rose, K. Guru Prasad, T. Sakthivel, V. Gunasekaran, T. Maiyalagan, and T. Vijayakumar, Electrochemical Analysis of Graphene Oxide/Polyaniline/Polyvinyl Alcohol Composite Nanofibers for Supercapacitor Applications. *Appl. Surf. Sci.* 449, 551 (2018).
34. Z. Xu, T. Wang, L. Wang, J. Xu, P. Liu, X. Lan, X. Li, M. Ni, Q. Jiang, and F. Jiang, Aniline-Grafting Graphene Oxide/Polyaniline Composite Prepared via Interfacial Polymerization with High Capacitive Performance. *Int. J. Energy Res.* (2019). https://doi.org/10.1002/er.4756.
35. S. Bilal, B. Begum, and S. Gul, PANI/DBSA/H_2SO_4: A Promising and Highly Efficient Electrode Material for Aqueous Supercapacitors. *Synth. Met.* 235, 1 (2018).
36. C.-H. Chen, J.-M. Wang, and W.Y. Chen, Conductive Polyaniline Doped with Dodecyl Benzene Sulfonic Acid: Synthesis, Characterization, and Antistatic Application. *Polymers (Basel).* 12, 2970 (2020).
37. Z. Çıplak, A. Yıldız, and N. Yıldız, Green Preparation of Ternary Reduced Graphene Oxide-Au@polyaniline Nanocomposite for Supercapacitor Application. *J. Energy Storage* 32, 101846 (2020).
38. R. Awata, M. Shehab, A. El Tahan, M. Soliman, and S. Ebrahim, High Performance Supercapacitor Based on Camphor Sulfonic Acid Doped Polyaniline/Multiwall Carbon Nanotubes Nanocomposite. *Electrochim. Acta* 347, 136229 (2020).
39. R. Bortamuly, G. Konwar, P.K. Boruah, M.R. Das, D. Mahanta, and P. Saikia, CeO_2-PANI-HCl and CeO_2-PANI-PTSA Composites: Synthesis, Characterization, and Utilization as Supercapacitor Electrode Materials. *Ionics (Kiel).* 26, 5747 (2020).
40. A. Viswanathan, and A.N. Shetty, The High Energy Supercapacitor from RGO/Ni$(OH)_2$/PANI Nanocomposite with Methane Sulfonic Acid as Dopant. *J. Colloid Interface Sci.* 557, 367 (2019).
41. N.R. Dywili, A. Ntziouni, C. Ikpo, M. Ndipingwi, N.W. Hlongwa, A.L.D. Yonkeu, M. Masikini, K. Kordatos, and E.I. Iwuoha, Graphene Oxide Decorated Nanometal-Poly(Anilino-Dodecylbenzene Sulfonic Acid) for Application in High Performance Supercapacitors. *Micromachines* 10, 115 (2019).
42. H. Gul, A.U.H.A. Shah, U. Krewer, and S. Bilal, Study on Direct Synthesis of Energy Efficient Multifunctional Polyaniline-Graphene Oxide Nanocomposite and Its Application in Aqueous Symmetric Supercapacitor Devices. *Nanomaterials* 10, 118 (2020).
43. H. Gul, A.H.A. Shah, and S. Bilal, Fabrication of Eco-Friendly Solid-State Symmetric Ultracapacitor Device Based on Co-Doped PANI/GO Composite. *Polymers (Basel).* 11, 1315 (2019).
44. L. Fan, L. Yang, X. Ni, J. Han, R. Guo, and C. Zhang, Nitrogen-Enriched Meso-Macroporous Carbon Fiber Network as a Binder-Free Flexible Electrode for Supercapacitors. *Carbon N. Y.* 107, 629 (2016).
45. J. Niu, R. Shao, J. Liang, M. Dou, Z. Li, Y. Huang, and F. Wang, Biomass-Derived Mesopore-Dominant Porous Carbons with Large Specific Surface Area and High Defect Density as High Performance Electrode Materials for Li-Ion Batteries and Supercapacitors. *Nano Energy* 36, 322 (2017).
46. F. Soysal, Z. Çıplak, B. Getiren, C. Gökalp, and N. Yıldız, Synthesis and Characterization of Reduced Graphene Oxide-Iron Oxide-Polyaniline Ternary Nanocomposite and Determination of Its Photothermal Properties. *Mater. Res. Bull.* 124, 110763 (2020).
47. F. Soysal, Z. Çıplak, B. Getiren, C. Gökalp, and N. Yıldız, Synthesis of GO-Fe3O4-PANI Nanocomposite with Excellent NIR Absorption Property. *Colloids Surf. A Physicochem. Eng. Asp.* 578, 123623 (2019).
48. D. Shi, C. Wei, F. Duan, and M. Chen, Fabrication of Uniform Nanocomposite by "Anchoring" Polyaniline Nanofibers on the Surface of Graphene Oxide for Supercapacitors. *Integr. Ferroelectr.* 161, 76 (2015).
49. N.P.S. Chauhan, M. Mozafari, N.S. Chundawat, K. Meghwal, R. Ameta, and S.C. Ameta, High-Performance Supercapacitors Based on Polyaniline-Graphene Nanocomposites: Some Approaches, Challenges and Opportunities. *J. Ind. Eng. Chem.* 36, 13 (2016).
50. M.D. Stoller, and R.S. Ruoff, Best Practice Methods for Determining an Electrode Material's Performance for Ultracapacitors. *Energy Environ. Sci.* 3, 1294 (2010).
51. H. Li, J. Wang, Q. Chu, Z. Wang, F. Zhang, S. Wang, E. Frackowiak, V. Khomenko, K. Jurewicz, K. Lota, F. Béguin, U. Male, J.K.R. Modigunta, D.S. Huh, M. Manoj, K.M. Anilkumar, B. Jinisha, S. Jayalekshmi, S. Mondal, U. Rana, S. Malik, M.D. Stoller, R.S. Ruoff, T.C. Girija, M.V. Sangaranarayanan, S. Cho, K.H. Shin, J. Jang, Y. Gao, J. Ying, X. Xu, L. Cai, Y. Yan, Q. Cheng, G. Wang, C. Li, R. Malik, L. Zhang, C. McConnell, M. Schott, Y.Y. Hsieh, R. Noga, N.T. Alvarez, and V. Shanov, Best Practice Methods for Determining an Electrode Material's Performance for Ultracapacitors. *J. Power Sources* 110, 242 (2017).
52. J. Yan, Z. Fan, T. Wei, W. Qian, M. Zhang, and F. Wei, Fast and Reversible Surface Redox Reaction of Graphene-MnO2 Composites as Supercapacitor Electrodes. *Carbon N. Y.* 48, 3825 (2010).
53. P. Sen, A. De, A.D. Chowdhury, S.K. Bandyopadhyay, N. Agnihotri, and M. Mukherjee, Conducting Polymer Based Manganese Dioxide Nanocomposite as Supercapacitor. *Electrochim. Acta* 108, 265 (2013).
54. P. Kumari, K. Khawas, S. Nandy, and B.K. Kuila, A Supramolecular Approach to Polyaniline Graphene Nanohybrid with Three Dimensional Pillar Structures for High Performing Electrochemical Supercapacitor Applications. *Electrochim. Acta* 190, 596 (2016).
55. J. Ma, S. Tang, J.A. Syed, D. Su, and X. Meng, High-Performance Asymmetric Supercapacitors Based on Reduced Graphene Oxide/Polyaniline Composite Electrodes with Sandwich-like Structure. *J. Mater. Sci. Technol.* 34, 1103 (2018).
56. X. Yan, J. Chen, J. Yang, Q. Xue, and P. Miele, Fabrication of Free-Standing, Electrochemically Active, and Biocompatible Graphene Oxide−Polyaniline and Graphene−Polyaniline Hybrid Papers. *ACS Appl. Mater. Interfaces* 2, 2521 (2010).
57. A. Rose, N. Raghavan, S. Thangavel, B. Uma Maheswari, D.P. Nair, and G. Venugopal, Investigation of Cyclic Voltammetry of Graphene Oxide/Polyaniline/Polyvinylidene Fluoride Nanofibers Prepared via Electrospinning. *Mater. Sci. Semicond. Process.* 31, 281 (2015).

58. E. Mitchell, J. Candler, F. De Souza, R.K. Gupta, B.K. Gupta, and L.F. Dong, High Performance Supercapacitor Based on Multilayer of Polyaniline and Graphene Oxide. *Synth. Met.* 199, 214 (2015).
59. D. Xu, Q. Xu, K. Wang, J. Chen, and Z. Chen, Fabrication of Free-Standing Hierarchical Carbon Nanofiber/Graphene Oxide/Polyaniline Films for Supercapacitors. *ACS Appl. Mater. Interfaces* 6, 200 (2014).
60. D. Kumar, A. Banerjee, S. Patıl, and A.K. Shukla, A 1 V Supercapacitor Device with Nanostructured Graphene Oxide/Polyaniline Composite Materials. *Bull. Mater. Sci.* 38, 1507 (2015).